Reverse Engineering, Additive Manufacturing, Point Cloud, Mesh, Reflectance

Elvis COUTIÑO-MORENO [0000-0003-2455-2574]*,
Quirino ESTRADA [0000-0003-0623-3780]**,
Daniel MALDONADO-ONOFRE [0000-0002-6078-2206]*,
Alejandro RODRIGUEZ-MENDEZ [0000-0002-5252-109X]***,
Julio GOMEZ-GIRON [0000-0003-4774-6486]****

RESOLUTION IN THE 3D MODELING OF OBJECTS FOR ADDITIVE MANUFACTURING AND REVERSE ENGINEERING – SHUTTER EFFECT

Abstract

This article presents a proportional relationship between Shutter and the value of the resolution scanning system that allows decision making for modeling 3D parts used in reverse engineering and additive manufacturing. As a first step, the object of interest is treated to dim excessive brightness, then the object is scanned (by point cloud or mesh) with the use of a Handyscan 700 scanner. The point cloud is processed with the Geomagic software Desing X to generate a CAD image and a ".stl" file for 3D printing.

1. INTRODUCTION

During the development of a new product, it is necessary to carry out a systematic analysis of the ideal manufacturing technique that will best adapt to the needs and budget of the customer (Akhmet & Fen, 2016; Ruan et al., 2016; Babel, Sawicki & Gasiorowski, 2021; Rojo, Bonilla & Masaquiza, 2018; Lan et al., 2018). The current demand for quality and low cost products has lead us into a new industrial revolution for manufacturing (Herrmann, 2002; Pedroza, 2018), where computer-aided design, CAD, software plays an important role in the design process. In the last three decades, the world has witnessed a digital transformation of every aspect of life and society. There exists a multitude of examples regarding this change: CAD, CAM, CAE systems, TDT, magnetic resonance, TAC, 3D ultrasound, etc (Bilal et al., 2020; Gonzalo, Sandra & Rodrigo, 2020). 3D scanning is among these techniques, which consists of capturing geometric information of a physical object by means of large capacity data acquisition tools such as laser scanners, optical digitizers, probes, contact arms, coordinate-measuring machines and computerized axial tomography scanners

* Jocotitlan Institute of Technology for Higher Education, elvis.coutino@tesjo.edu.mx, daniel.maldonado@tesjo.edu.mx
** Autonomous University of Ciudad Juarez, Technology and Engineering Institute, quirino.estrada@uacj.mx
*** University of California at Berkeley, Mechanical Engineering Department, aleromende@berkeley.edu
**** National Center for Research and Technological Development, Biomechatronics Engineering, juliogomez@cenidet.edu.mx

(Babel, Sawicki & Gasiorowski, 2021; Li, 2001). A 3D scanner can be defined as a device that analyses a real-world object or environment to collect data on its shape and possibly its appearance. The collected data can then be used to construct digital 3D models (Saorín et al., 2017; Montusiewicz, Czyz & Kayumov, 2015; Montusiewicz, Czyz & Kesik, 2015; Fines & Agah, 2008; Ojeda, Belete & Batista, 2014).

In this paper we establish a proportional relationship in the process of data acquisition, such that the data processing reduces the processing time during reverse engineering.

2. DEVELOPMENT

In this section, the process of digitization and CAD modeling of an object is presented.

2.1. 3D Digitization

The first step in reverse engineering consists in capturing the object's geometry. This is done by means of a Handyscan scanner shown in Fig. 1. More specifications of this scanner are given in Table 1.

Fig. 1. Handyscan 700 scanner

The following procedure was considered for the scanner's manipulation: 1. Hamdyscan 700 position. When scanning the object of interest, it is important to keep a distance of 12 in from the object. The scanner has poka-yoke LED that indicates the correct distance. The scan is done until a homogenous point cloud is obtained as seen in Fig 2.
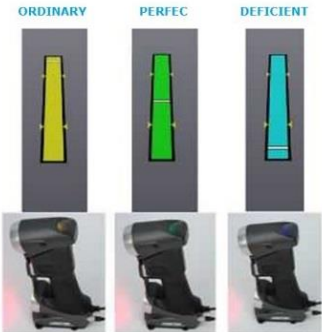
Fig. 2. Distance poka-yoke

**Tab. 1. Handyscan 700 technical specifications**

Specifications	Handyscan 700
Dimensions	122 x 77 x 294 mm
Scanning speed	480 000 measures/s
Scanning area	275 x 250 mm
Light source	7 transversal lasers (+1 additional line)
Laser type	II (safe for unintentional eye exposure)
Resolution	0.050 mm
Precision	Up to 0.030 mm
Volumetric accuracy	0.020 mm + 0.060 mm/m
Volumetric accuracy (with 3D Maxshot)	0.020 mm + 0.025 mm/m
Safety distance	300 mm
Depth of field	250 mm
Object size (Recommended)	0.1–4 m
Connection standard	1 USB port 3.0
Operation Temperature	15–40 °C
Operation Humidity (without condensation)	10.90% Figure 2.

Points of reference. The digitization process with a scanner includes preparation of the working table using stickers or reference points that provide a reference frame to capture the object's surface. The object's preparation depends on it size. Sticker are not required on small objects. For large objects, reference points must be located strategically in such a way that three of these points must always be aligned for surface recognition, as seen in Fig. 3.


Fig. 3. Object preparation

It is important to mention that due to surface characteristics, the scanner used in this work provides two different kinds of laser beams, as seen in Fig 4. The first type has a parallelogram pattern typically used for planar surfaces. For regions on the object's surface which have different depths and angular shapes it is convenient to use a linear laser beam.

| **a)** | **b)** |
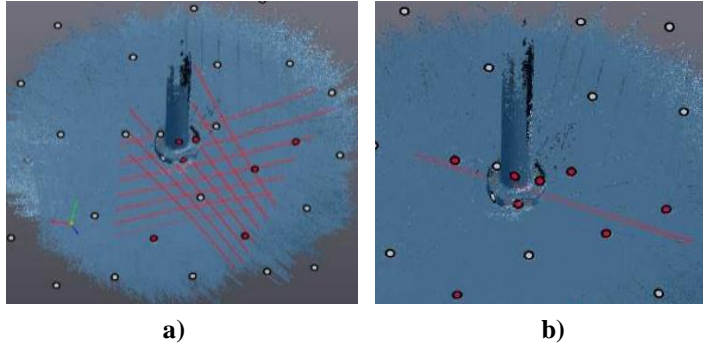
Fig. 4. a) Parallelogram laser pattern, b) linear laser

Point cloud (mesh). Information is captured and sent to the VXelements software. The result is one or several point clouds that represent the entire object. The point clouds may contain points that do not correspond to the object's surface geometry. The actual object that was digitized is shown in Fig. 5.
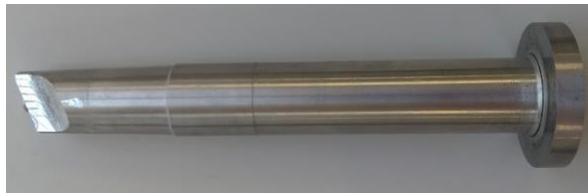

Fig. 5. Side bolt

The object's brightness is an important factor that must be considered during the scanning process, since it can cause problems while generating the point cloud as seen in Fig. 6 where it is observed that the object's shape is incomplete due to its brightness.
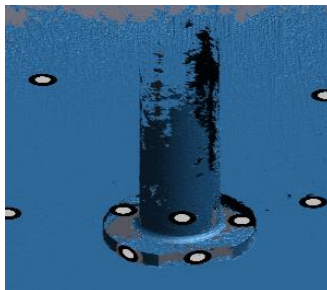
Fig. 6. Scanned object digitized in Xelements

For this purpose, it is recommended to apply white chalk on the object's surface to reduce its brightness (Fig. 7), thus minimizing distortion of the point cloud and reducing the total processing time.

|	
a)	**b)**
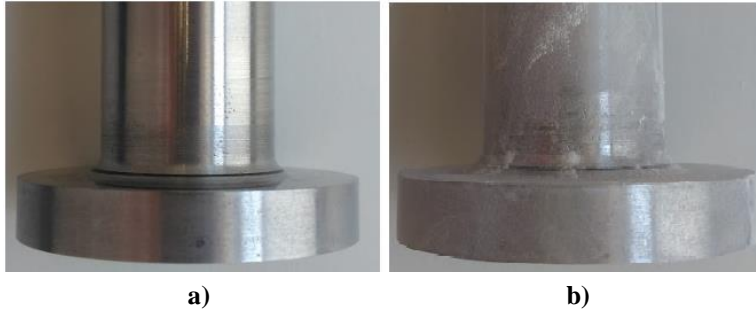
Fig. 7. Scanned object: a) high brightness, b) reduced brightness

One of the most important parameters while scanning an object is the shutter speed. The shutter regulates the frequency and intensity at which the laser is projected towards the object. The shutter must be adjusted according to the object's color.
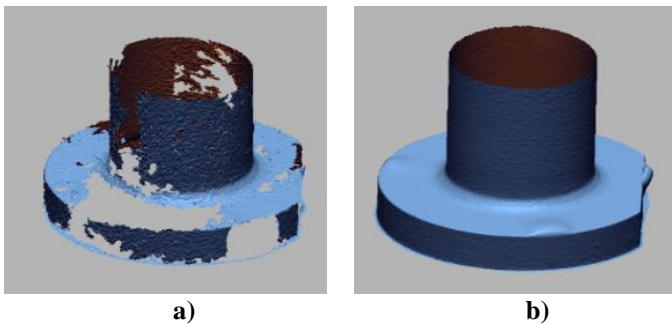
2.2. Point cloud processing

In Fig. 8 we observe that the point cloud has vortex regions in areas around holes, surfaces that are not completely defined and on the working table. Thus, we process the point cloud in order to eliminate all those points that do not belong to the desired object.

|	
a)	**b)**
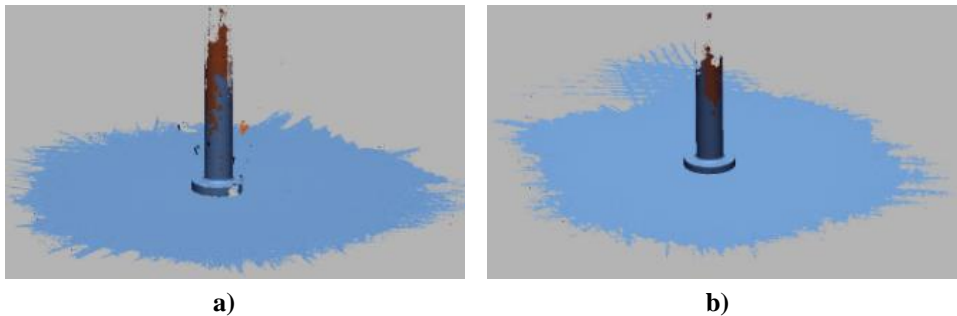
Fig. 8. Point cloud: a) high brightness, b) reduced brightness

The point cloud is further processed by smoothing all even surfaces and breaking the piece in segments for easier visualization. As observed in Fig. 9, the point cloud is better defined when the object's surface was treated to reduce its brightness, hence reducing the processing time and increasing accuracy in the design of the CAD model.

a)	**b)**

Fig. 9. Processed point cloud: a) high brightness, b) reduced brightness

It is necessary to mention that the point cloud is not yet a solid, it only serves as a reference for the CAD drawing. We also observe that after segmentation, the object is also better defined when its surface was treated to reduce brightness, as seen in Fig. 10.

a)   b)
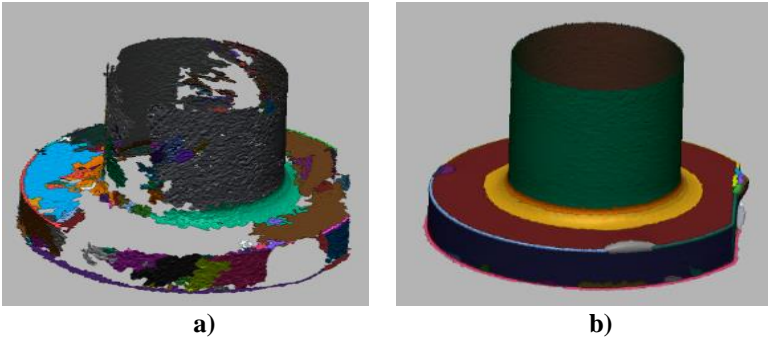
Fig. 10. Segmented point cloud: a) high brightness, b) reduced brightness

2.3. CAD drawing

Once the processing and cleaning of the point cloud is done, we proceed to create the CAD drawing using the Geomagic Desing X software. To make the drawing, we take as reference those lines generated by the point cloud (Fig. 11) in order to keep the lines in the drawing close to the digitized ones, thus obtaining a good approximation to the original dimensions.

a)   b)   c)
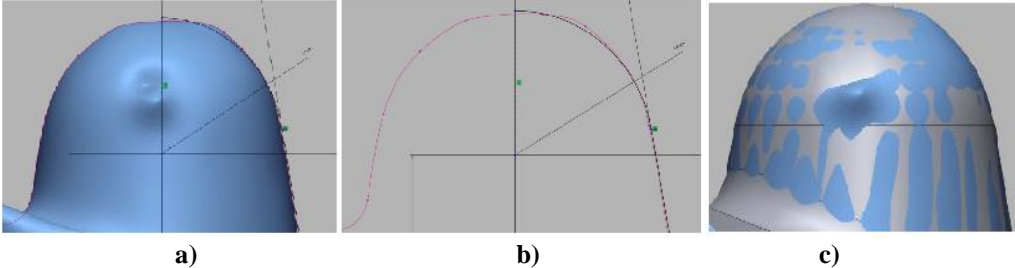
Fig. 11. Sketch generation a) point cloud, b) reference lines, c) CAD model

The drawing allows for the object's dimensions to be modified. The objects geometry may be improved and corrected if necessary. In Fig. 12 we observe the CAD model of the object presented previously in Fig. 5. The model can be converted to several formats for its use by software such as Solidworks and other applications.
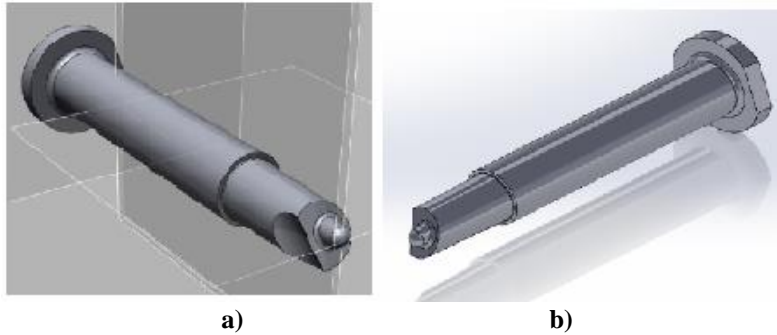
a)   **b)**

Fig. 12. CAD model in a) Geomagic Desing X, b) Solidworks

2.4. 3D printing

One of the advantages of digitizing a piece is the capacity to manufacture it by 3D printing as many times as necessary. For the purpose of this study we printed only a segment of the object as seen in Fig. 13.
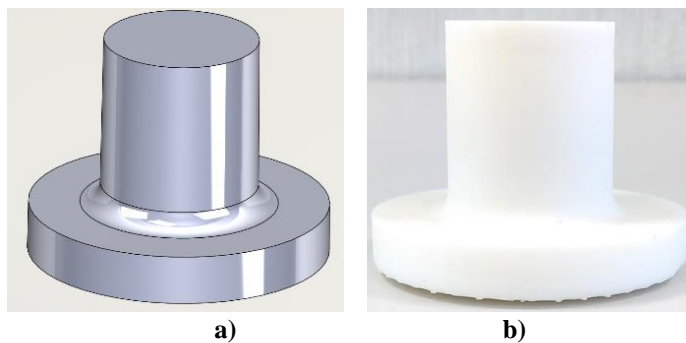

a)   **b)**

Fig. 13. a) CAD model, b) 3D printed object

3. RESULTS AND DISCUSSION

As mentioned above, excessive brightness of the object may complicate the digitization of its surface. For this purpose, we do 24 test scans where we modify the scanning resolution and the shutter speed on the object with and without brightness. The qualitative and quantitative results are presented below. We also compare the final dimensions of the physical object with the CAD model and the 3D printed piece.

3.1. Brightness effect on the scanning process

Fig. 14 presents the object's dimensions that will be analyzed in this work.
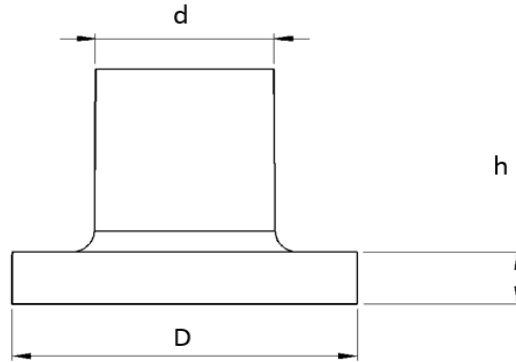
Fig. 14. Measures

Tables 2 and 3 show the results obtained during scanning at different surface conditions (with and without brightness), resolution (0.2, 0.5 and 1 mm) and shutter (0.6, 2.6, 4.6, 6.6). From Table 2 we observe that the dimension variability for the part with full brightness is of 0.183–1.917%, 0–0.5% and 0.708–5.272% for dimensions D, d and h respectively. On the other hand, for the part without brightness, we obtained ranges in the order of 0.03–0.05%, 0.223–1.817%, 1.13–7.39% for dimensions D, d and h respectively. Hence, we observe that the part without chalk has larger data dispersion than the part with chalk. This trend also occurs for all values of shutter speed. Considering the D dimension, a shutter speed of 0.6, 4.6, and 6.6 yields a dispersion of 0.045–1.017%, 1.334–2.367% and 0.033–1.634% respectively for the part with brightness and 0.183–0.934%, 0.33–1% & 0.033–0.367% respectively for the part without brightness.

Fig. 16 shows the D dimension variability for a shutter speeds of 2.6 (for shutter speeds of 0.6, 4.6 & 6.6 see Fig. 15, Fig. 17 and Fig. 18) in order to visualize trends and difference between the parts with and without brightness. From Fig. 16 we observe that the part with brightness shows higher variability percentage at a higher resolution due to laser scattering from the surface of the part. This high reflectance of the material causes some features on the object's surface not to be recognized, thus we obtain a larger error between the dimensions of the point cloud and the physical object.

Tab. 2. Shutter value 0.6 and 2.6

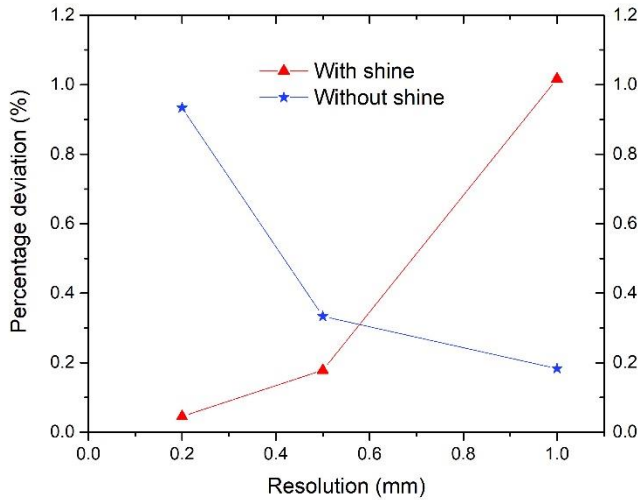| Shutter 0.6						
Resolution (mm)	**Dimension**	**Physical part**	**Dimensions (mm) CAD**		**Diference between phiysical and CAD models (%)**	
			Whit glow	**No glow**	**Whit glow**	**No glow**
0.2	D	59.980	60.007	60.540	0.045	0.934
	d	31.370	31.390	31.290	0.065	0.255
	h	10.000	10.436	9.974	4.360	0.258
0.5	D	59.980	59.873	60.180	0.178	0.333
	d	31.370	31.240	31.370	0.414	0.000
	h	10.000	9.049	9.791	9.511	2.086
1	D	59.980	60.590	59.870	1.017	0.183
	d	31.370	31.200	31.300	0.542	0.223
	h	10.000	10.500	9.799	5.000	2.015
Shutter 2.6						
0.2	D	59.980	58.830	60.000	1.917	0.033
	d	31.370	31.370	31.200	0.000	0.542
	h	10.000	9.473	9.887	5.272	1.135
0.5	D	59.980	59.870	60.000	0.183	0.033
	d	31.370	31.210	31.300	0.510	0.223
	h	10.000	10.071	9.748	0.708	2.520
1	D	59.980	59.750	59.950	0.383	0.050
	d	31.370	31.460	30.800	0.287	1.817
	h	10.000	10.454	9.261	4.535	7.393

Fig. 15. Shutter value graph 0.6

Tab. 3. Shutter value 4.6 and 6.6

| Resolution (mm)	Dimension	Physical part	Dimensions (mm) CAD		Diference between phiysical and CAD models (%)	
			Whit glow	No glow	Whit glow	No glow
Shutter 4.6						
0.2	D	59.980	59.180	60.040	1.334	0.100
	d	31.370	31.300	31.200	0.223	0.542
	h	10.000	9.830	9.875	1.700	1.246
0.5	D	59.980	59.840	60.000	0.233	0.033
	d	31.370	31.400	30.400	0.096	3.092
	h	10.000	9.970	9.636	0.300	3.641
1	D	59.980	58.560	60.000	2.367	0.033
	d	31.370	31.000	30.600	1.179	2.455
	h	10.000	9.570	9.283	4.300	7.172
Shutter 6.6						
0.2	D	59.980	59.920	60.000	0.100	0.033
	d	31.370	31.400	31.200	0.096	0.542
	h	10.000	9.750	10.000	2.500	0.000
0.5	D	59.980	60.000	60.000	0.033	0.033
	d	31.370	31.200	31.200	0.542	0.542
	h	10.000	9.410	9.660	5.900	3.400
1	D	59.980	59.000	60.200	1.634	0.367
	d	31.370	31.200	31.200	0.542	0.542
	h	10.000	10.000	9.600	0.000	4.000
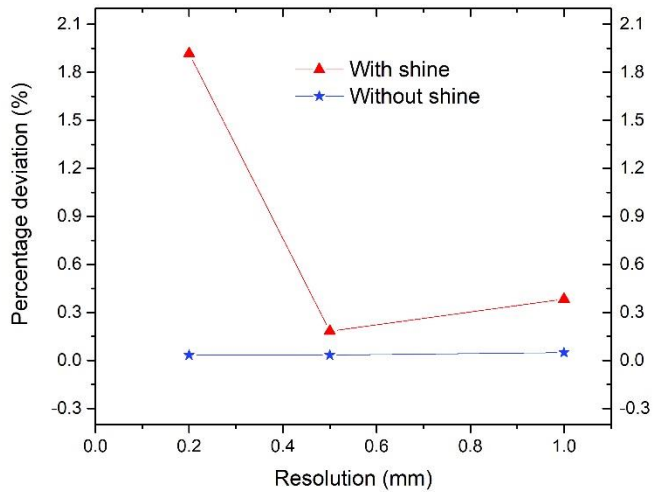
Fig. 16. Shutter value graph 2.6

In the case of the part with chalk, the D dimension variability is lower with higher resolution since the laser is stable on the surface of the object due to its lower reflectance relative to other optical properties. This behavior occurs for all the values of shutter speed studied in this article.
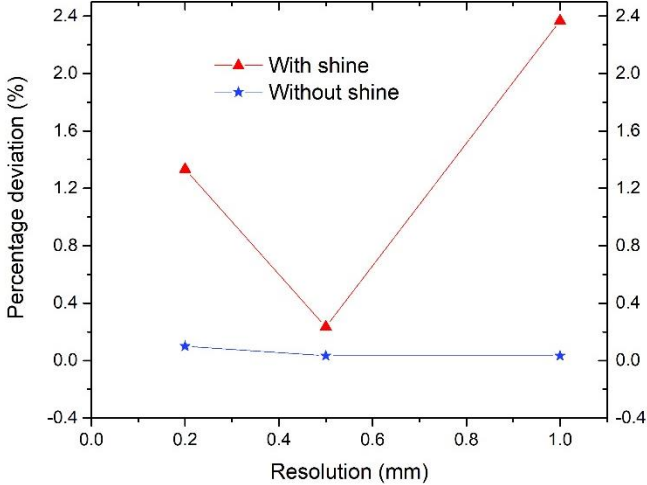
Fig. 17. Shutter value graph 4.6
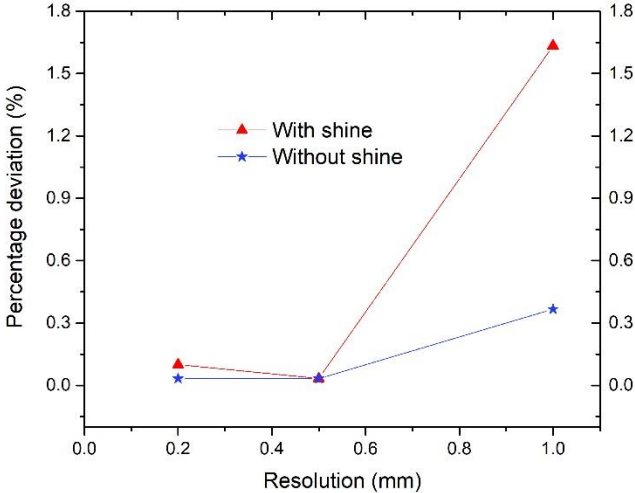
Fig. 18. Shutter value graph 6.6

Lastly, from previous results (See Fig. 15–18) the importance of the resolution by shutter effects was demonstrated. Regardless the shine condition, and for the specific case of this article, the lowest difference (0.6%) between the physical part and the point cloud dimensions was calculated when at resolution of 0.5 is selected.

4. CONCLUSIONS

In this work we scanned a bright object whose surface was dimed to minimize its optical reflectance thus obtaining a geometric approximation of the object within 99.9% of its morphologic characteristics such as smoothness and dimensions. For white color we used a shutter speed of 2.6 and 2.5 mm of resolution. With these parameters, the difference relative to the original object was of 0.033%. For the parts with a high reflectance index, we propose a combination of $2.6 - 4.6$ in shutter speed with a resolution of 0.5 mm. Finally, respect to original dimensions, a cumulative error less than 1% was obtained during the scanning and digitizing process of the part.

Acknowledgment

REFERENCES

Akhmet, M., & Fen, M. O. (2016). Unpredictable points and chaos. *Communications in Nonlinear Science and Numerical Simulation*, *40*, 1–5. http://doi.org/10.1016/j.cnsns.2016.04.007

Babel, R., Sawicki, K., & Gasiorowski, M. (2021). Obtaining the 3D geometry of the blade in a training aircraft. *Journal of Physics: Conference Series*, *1736*, 012047. http://doi.org/10.1088/1742-6596/1736/1/012047

Bilal, M., Neha, S., Shuaishuai, C., Florian, S., Hans-Florian, Z., & Florian, M. (2020). Evaluation of the Dimensional Accuracy of 3D-Printed Anatomical Mandibular Models Using FFF, SLA, SLS, MJ, and BJ Printing Technology. *Journal of Clinical Medicine*, *9*, 1–18. http://doi.org/10.3390/jcm9030817

Fines, J. M., & Agah, A. (2008). Machine tool positioning error compensation using artificial neural networks. *Engineering Applications of Artificial Intelligence,* *21*(7), 1013–1026. http://doi.org/10.1016/j.engappai.2007.10.001

Gonzalo, T., Sandra, B., & Rodrigo, L. (2020). Three-dimensional Virtual Models of 3D-Scanned Real Cadaveric Samples Used as a Complementary Educational Resource for the Study of Human Anatomy: Undergraduate Student's Perception of this New Technology. *International Journal of Morphology*, *38*(6). http://dx.doi.org/10.4067/S0717-95022020000601686

Herrmann, R. K. (2002). Linking theory to evidence in international relations. In W. Carlsnaes, T. Risse & B. A. Simmons (Eds.), *Handbook of international relations* (pp. 119–136). Sage.

Lan, L., Longfei, Y., Fei, Y., Jianping, S., Liya, Z., Xianfeng, Y., Huajian, T., & Xingsong, W. (2018). 3D printing individualized heel cup for improving the self-reported pain of plantar fasciitis. *Journal of Translational Medicine*, *16*, 1–11. https://doi.org/10.1186/s12967-018-1547-y

Li, X. (2001). Real-time prediction of workpiece errors for a CNC turning centre, Part 1. Measurement and identification. *International Journal of Advanced Manufacturing Technology,* *17*(9), 649–653. http://doi.org/10.1007/s001700170128

Montusiewicz, J., Czyz, Z., & Kayumov, R. (2015). Selected methods of making three-dimensional virtual models of museum ceramic objects. *Applied Computer Science*, *11*(1), 1–16.

Montusiewicz, J., Czyz, Z., & Kesik, J. (2015). Using 3D replication technology in preparing didactic aid sets in the area of cultural heritage. In L. Gomez Chova, A. Lopez Martinez & I. Candel Torres (Eds.), *EDULEARN 15: 7th International Confrence on Education and New Learning Technologies* (pp. 1861–1871). IATED Academy.

Ojeda, P. F., Belete, F. O., & Batista, L. Y. (2014). Elaboración del modelo digital de elevaciones mediante tecnología 3D láser escáner. *Minería y Geología*, *30*(1), 95–103.

Pedroza, F. R. (2018). A universidade 4.0 com currículo inteligente 1.0 na quarta revolução industrial. *RIDE Revista Iberoamericana Para La Investigación Y El Desarrollo Educativo*, *9*(17), 168–194. https://doi.org/10.23913/ride.v9i17.377

Rojo, G. A., Bonilla, J. D., & Masaquiza, C. C. (2018). The development of new products and their impact on production: Case study BH Consultores. *Scielo*, *10*(1), 1–5.

Ruan, B., Li, G. Q., Chen, Y., Mitrouchev, P., He, B., & Lu, L. X. (2016). New tension mechanism for high-speed tensile testing machine. *International Journal of Automotive Technology*, *17*(6), 1033–1043. http://doi.org/10.1007/s12239-016-0101-2

Saorín, J. L., Meier, C., de la Torre-Cantero, J., Carbonell-Carrera, C., Melián-Díaz, D., & Bonnet de León, A. (2017). Competencia Digital: Uso y manejo de modelos 3D tridimensionales digitales e impresos en 3D. *EDMETIC*, *6*(2), 27–46. https://doi.org/10.21071/edmetic.v6i2.6187